



Journal of Agrometeorology

ISSN : 0972-1665 (print), 2583-2980 (online)

Vol. No. 26 (3) : 279-289 (September - 2024)

<https://doi.org/10.54386/jam.v26i3.2589>

<https://journal.agrimetassociation.org/index.php/jam>



Research Paper

Influence of atmospheric stability conditions on wind energy density in Ali Al-Gharbi region of Iraq

JAFAR MOHAMMED KHADIR*¹, AHMED F. HASSOON¹ and BASIM ABDULSADA AL-KNANI¹

¹Department of Atmospheric Sciences, College of Science, Mustansiriyah University, Baghdad, Iraq

*Corresponding author e-mail: jafar941@uomustansiriyah.edu.iq

ABSTRACT

Atmospheric stability is considered as one of the most important factors affecting the increase or decrease in wind speed in the atmosphere and thus affects the wind energy density. This study aims to analyze the stability of the atmospheric conditions in southern part of Iraq, specifically in the Ali Al-Gharbi region, using one of methods to determine atmospheric stability called Monin-Obukhov length. Field data of horizontal and vertical wind speed and air temperature collected at three heights (10m, 30m, and 50m) in 2017 from tower installed in Ali Al-Gharbi region. The results show that the vertical wind speed increases with height up to 30 m and decreases at 50 m, while the horizontal wind speed increases as the height increases. The friction velocity, surface heat flux, momentum flux and shear stress were calculated and the stability conditions were determined. Results revealed that stable atmospheric condition was the most frequent with about 59% occasions occurring during the year followed by unstable (40%) and neutral (1%) conditions. The highest wind energy density was in stable conditions ($0 \leq L < 200$), with percentage (58% - 57%) in spring season at both heights 10m and 50m, respectively, followed by unstable conditions ($-200 < L \leq 0$), while the lowest wind energy density was in neutral conditions ($-200 \leq L \leq 200$) with percentage (1.3% - 0.8%) in autumn season.

Keywords: Atmospheric stability, Wind power energy, Monin-Obukhov length, Surface heat flux, Momentum flux.

The world is moving towards renewable energy (green, alternative, or environmentally friendly energy) in the use and consumption of energy (Hassan *et al.*, 2024). Green energy sources are clean, environmentally friendly, and renewable, and do not emit harmful gases that pollute the environment, such as carbon dioxide, nitrogen dioxide, and methane, and since their source are natural, they are not exhausted (Singh *et al.*, 2021). Renewable energies have the potential to provide relatively clean energy (Hadi *et al.*, 2020). Renewable energy generation and its technologies have different sources, such as wind energy, sun energy, ocean energy, biomass, hydropower, and geothermal energy resources (Munjong, 2022). Wind energy has recently been considered one of the fastest-growing energy sources due to its numerous applications and advantages. Most energy-generating stations require large amounts of water and wind energy does not require water to generate (Nwaigwe, 2021).

The most important parameter that must be taken into consideration when designing and studying wind power conversion systems is wind speed (Hadi *et al.*, 2020). Wind energy production

is best suited to areas with strong wind speeds and moderate turbulence intensity (Pérez *et al.*, 2023). The convective layer is a turbulent layer that affects horizontal wind movement and wind energy (Hassoon and Roomi, 2023). The quantity of turbulence that occurs in the atmosphere relates to the stability of the atmosphere (Radünz *et al.*, 2020). Atmospheric stability can be divided into three categories: stable, neutral, and unstable, in unstable conditions, extensive mixing occurs in atmospheric layers, leading to a smaller difference in wind speed and temperature, while in stable conditions, mixing is limited in the layers, under neutral conditions, mixing is equal, which leads to maintaining constant temperature gradients and wind speed in the atmosphere (Pérez *et al.*, 2023). Meteorological factors affecting wind speed estimation, such as turbulent intensity, atmosphere stability, surface roughness, and wind shear, all these factors characterize the surface layer, and these characteristics usually assume a neutral atmosphere, which leads to changes in the predicted wind speed, and effects on energy production.

Article info - DOI: <https://doi.org/10.54386/jam.v26i3.2589>

Received: 7 May 2024; Accepted: 6 June 2024; Published online : 01 September 2024

"This work is licensed under Creative Common Attribution-Non Commercial-ShareAlike 4.0 International (CC BY-NC-SA 4.0) © Author (s)"

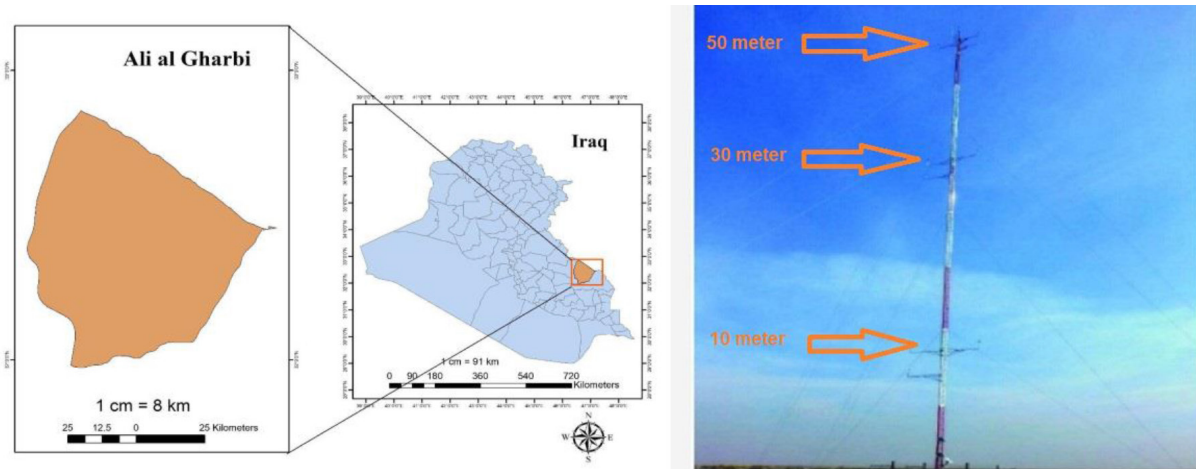


Fig. 1: Location of the study area and the meteorological 50 m tower at Ali Al-Gharbi meteorological station

The Monin–Obukhov Similarity Theory (MOST) determines the mean flow and mean temperatures in the surface layer under non-neutral conditions as a dimensionless function of height. The logarithmic wind profile for the neutral boundary layer will be obtained by applying the mixed-length theory, which states that the height logarithm is proportional to the horizontal component of the mean flow. By characterizing vertical distributions of average flow and temperature through known “universal functions” of dimensionless height, (MOST) further generalizes the mixing length theory under non-neutral situations. A major advancement in contemporary micrometeorology was the development of the MOST, which served as the theoretical foundation for several micrometeorological experiments and measuring methods (Stiperski and Calaf, 2023).

Pérez *et al.*, (2023) explained that there was a clear relationship between atmospheric stability and energy generation in wind farms and showed that the fluctuation in atmospheric stability conditions led to large differences in the estimation of energy production. Abdalla *et al.*, (2023) studied atmospheric stability and its impact on wind power density for an entire year and showed that the stable atmospheric condition dominated in all seasons and ignoring it impacted the accuracy of estimating wind power density. Resen (2023) conducted a wind resource assessment for the Ali Al-Gharbi site and found that the Ali Al-Gharbi is the most suitable region in southern Iraq for wind energy production. This study aims to determine seasonal stability cases using the Monin-Obukhov method and study its impact on wind energy productivity.

MATERIALS AND METHODS

Study location and observations

Ali Al-Gharbi city is 110 km northeast of Amara province and is located at longitude of 46.6878°E, latitude of 32.4617°N and situated at an altitude of 44 meters above sea level. Ali Al-Gharbi region is considered as one of the most promising areas in terms of producing electrical energy using wind turbines. A 50-meter tower was erected by the Ministry of Science and Technology for Scientific Research, Iraqi government at Ali Al-Gharbi to monitor and evaluate weather parameters as a part of the projects of wind

energy and the construction of wind farms mission (Fig. 1).

The meteorological parameters recorded at the meteorological tower station were wind speed (vertical and horizontal) and its direction, temperature, in addition to other parameter (neglected in this study) such as relative humidity, pressure, radiation intensity, and rainfall, etc. at 10-minute intervals and three heights (10, 30 and 50 meters). The devices installed on meteorological tower were Stylistis-100 loggers from the Greek company (Symmetron), and sensors from the American company (Renewable NRG Systems). Table 1 describes details sensor type, time interval, accuracy etc. The current study is considered part of many academic studies that addressed the impact of the issue of atmospheric stability on the intensity of wind energy production.

Determining atmospheric stability conditions

In order to determine the atmospheric stability conditions during the year we followed the Monin-Obukhov Similarity Theory. And to determine the Monin-Obukhov length (L) the wind shear stress, frictional velocity and sensible heat flux were computed as described below;

Shear stress

Stress is defined as the force of friction exerted per unit area, and this force is parallel to the surface. One of the types of stress used in atmospheric sciences is shear stress, which is given by the following equation (Kumar, 2022):

$$\tau = \rho u_*^2 \quad (1)$$

Where (ρ) is the air's density of 1.2 kg m⁻³, and (u_*) is the friction's velocity. The friction's velocity (u_*) is determined by the following formula (Roomi, 2000):

$$u_* = \sqrt{\left(\frac{\tau}{\rho}\right)} \quad (2)$$

Where (τ) represents the shear stress. In most meteorological applications, the shearing stress can be assumed irrespective of height in the shallow layer and hence equal to its value at the surface (Roomi, 2000).

Table 1: Specifications of the sensors installed in Ali Al-Gharbi meteorological tower

Sensor type	Parameter	Country of manufacture	Time interval	Accuracy	Sensor range
NRG 110SC (4429)	Air temperature	USA	10 minutes	$\pm 0.43 \text{ C}^\circ$	(-40 C°) to (65 C°)
NRG #40C	Horizontal wind speed	USA	10 minutes	$\pm 0.15 \text{ m s}^{-1}$	(0.33 m s^{-1}) to (24 m s^{-1})
RMY 27106T_C	Vertical wind speed	USA	10 minutes	$\pm 0.1 \text{ m s}^{-1}$	$\pm 15 \text{ m s}^{-1}$

$$u_* = \sqrt{\left(\frac{u}{\rho}\right)} = \sqrt{u'w'} \quad (3)$$

Assuming that (u') and (w') are simply equivalent in size, it can be concluded that (u_*) represents the amplitude of velocity changes in turbulent layer flow (Foken and Mauder, 2024). Particular instruments can calculate (u_*) directly by measuring (u), such as Gill's and Drag anemometers (Phillips *et al.*, 2021).

Sensible heat flux

Heating flux, often known as sensible heat, is the transfer of heat from the earth's surface to the atmosphere. Typically, this amount is 1/3 to 1/2 of the heat absorbed by sunlight at the surface, with the remainder shared between heat conserved in the earth and the heating required to evaporate liquid from soil and vegetation (Fiorillo *et al.*, 2023). The sensible heat flux is calculated by determining the turbulent changes in vertical wind velocity and temperature as in the equation (Roomi, 2000):

$$H = c_p \rho \overline{w'T'} \quad (4)$$

Where (w) represents vertical velocity, (T) is the temperature, and (c_p) is the specific heat at a constant pressure. The overbar represents a temporal average, whereas the prime denotes variation from the averaged quantity, and the average is considered as the average covariance between the temperature turbulent part and the vertical turbulent part (Morrison *et al.*, 2021).

Monin-Obukhov similarity theory (MOST)

The Monin-Obukhov length (L) is the most widely utilized aspect ratio for atmospheric stability. It is defined as a scale parameter, because it indicates the relationship between mechanics and convective turbulent production. (L) is calculated using the equation as follows (Hassoon and Al-Dabbagh, 2023; Göçmen *et al.*, 2016):

$$L = - \frac{c_p \rho T u_*^3}{k g H} \quad (5)$$

Where (T) is the mean surface layer temperature, (k) is a von Karman constant (0.4), and (H) is the sensible heat flow (Holtslag *et al.*, 2014). The classification of atmospheric stability according to The Monin-Obukhov length (L) method used in this study were stable ($0 \leq L < 200$), unstable ($-200 < L \leq 0$), and neutral ($-200 \leq L \leq 200$) (Roomi, 2000).

Wind power density (WPD)

Power density refers to the amount of power generated per unit area of the turbine's rotor-swept area. (WPD) is determined in (W m^{-2}) and can be calculated by the following equation (Al-Knani, 2015):

$$WPD = \frac{1}{2} \rho \quad (6)$$

Where (ρ) represents air density and (u) represents horizontal wind speed. Wind power is not entirely efficient, with a theoretical maximum mechanical efficiency of only 59.3% for turbines. In the present research, we will compute and identify the wind power density and wind classification at various heights (30m, and 50m).

Wind energy density

Energy estimation at a chosen location is one of the most crucial phases in wind energy projects. The standard used to assess the site's energy potential is typically the amount of wind energy that is accessible within the regime across time (Al-Knani, 2015). Energy can be expressed as the following equation:

$$E = (WPD) T_i \quad (7)$$

Where (T_i) represents the period; for instance, (T_i) equals (720) hours for a monthly length, or (8760) hours for an annual duration.

RESULTS AND DISCUSSION

Relationship between horizontal and vertical wind speed

The horizontal and vertical wind speed recorded at 10-min interval was transformed to daily average from January 1 to December 31 of year 2017 and are presented in Fig. 2 (a, b, c). The vertical wind speed increases with a height from about 0.06 m s^{-1} at 10m height to 0.28 m s^{-1} at 30m and decreases to 0.12 m s^{-1} at 50m height. The standard deviation of vertical wind speed was higher ($\pm 0.9 \text{ m s}^{-1}$) at 50m than that at 30m ($\pm 0.17 \text{ m s}^{-1}$). The horizontal wind speed component on an average was an order higher than the vertical wind speed component and increased with height with values of 3.5 m s^{-1} , 5.0 m s^{-1} and 5.7 m s^{-1} at 10m, 20m and 30m heights respectively. Its fluctuations were 0.06 m s^{-1} , 0.2 m s^{-1} and 0.1 m s^{-1} at height 10m, 30m and 50m respectively showing highest at 30m height.

The relation between horizontal and vertical components of winds are better explained through scattered plots (Fig 3). The behavior of change in vertical and horizontal wind at 30m is more explained clearly (Fig. 3 b) with a high value of correlation coefficient (0.976) which indicate that as the horizontal wind speed increases the vertical wind component proportionally increases. The correlation coefficients between two components of winds are 0.559 at 10m and 0.695 at 50m. This height of 30m is considered as the transfer zone between the friction layer and the interval layer in upper air when horizontal wind speed becomes accelerated to a height speed of about 14 m s^{-1} in 50m at this location see (Fig. 2 c). The relations developed (Fig. 3) characterize the very important effect on the selected height to install the turbine and to study the effect of stability on wind energy productivity.

Shear stress and friction velocity

Friction velocity known as the velocity of the eddy, this eddy is very significant in the turbulent assessment, its results from the differences and fluctuation of horizontal wind speed with height, also vertical wind speed. Thus, friction velocity depends on the wind speed value, most horizontal velocity transforms to downward, this downward flow caused stress and pressure on the ground surface and this stress resulted from mechanical turbulence and shear velocity. Eddy velocity or shear velocity calculation is particularly important on wind turbine blades because it will move this blade to produce electric electricity. The horizontal wind speed and friction velocity recorded during January to December 2017 at three heights are presented in Fig.4.

The horizontal wind speeds were $3.5 \pm 2.9 \text{ m s}^{-1}$, $5.0 \pm 3.2 \text{ m s}^{-1}$ and $5.7 \pm 3.5 \text{ m s}^{-1}$ respectively at 10m, 30m and 50m

heights. The friction velocity was $0.13 \pm 0.11 \text{ m s}^{-1}$ and $0.1 \pm 0.08 \text{ m s}^{-1}$ s at height 30m and 50m respectively (Fig. 4 b & c). The large fluctuation in friction velocity depends on roughness and convective conditions, according to that, there isn't a clear relationship between horizontal wind speed compound and friction velocity at 10 m height.

Air temperature and surface heat flux

Air temperature has a significant effect on the horizontal wind speed, because the moving air parcel has large acceleration to the upward restricted horizontal movement air mass parcel. Vertical movement, and sensible heat flux, considered one of the causes of instability and atmospheric turbulence. Surface heat flux is positive during the daytime and moves upward, while it's negative at nighttime and moves downward. The sensible heat flux based on homogeneous recorded data shows that when there is a

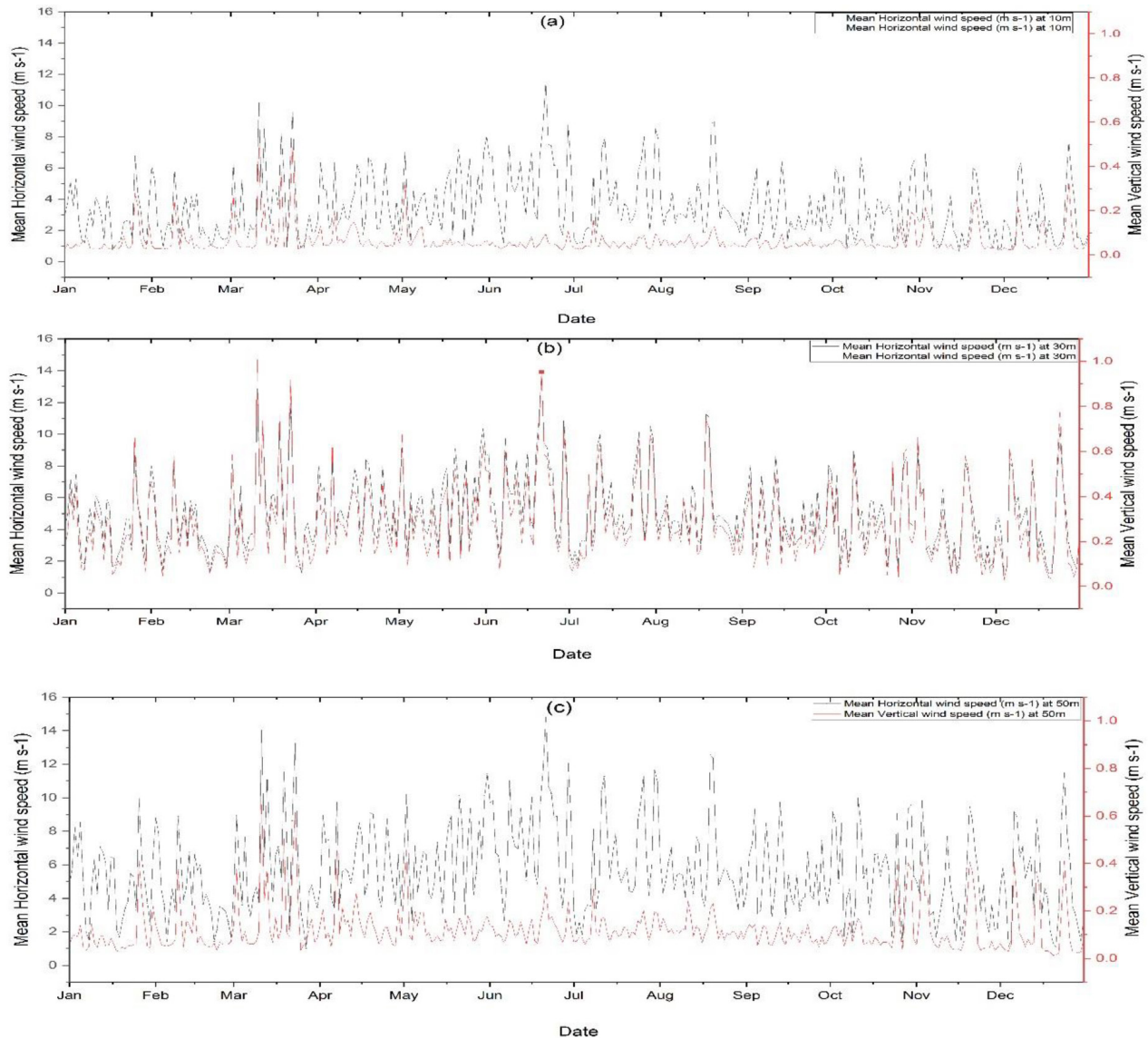


Fig. 2: Time series for horizontal and vertical wind speed at heights (a) 10m, (b) 30m, and (c) 50m during January to December 2017 at Ali Al-Gharbi Iraq.

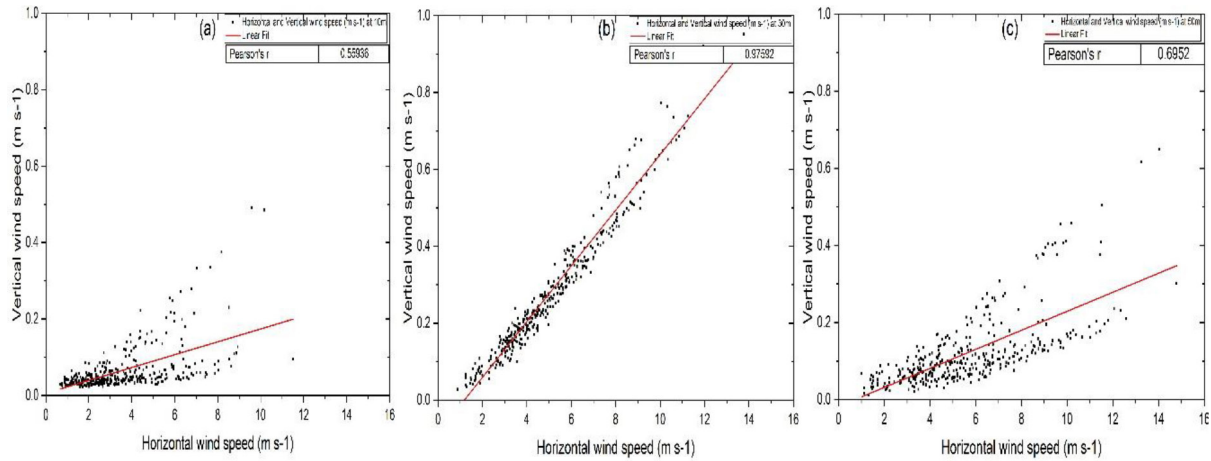


Fig. 3: Relationship between horizontal and vertical wind speed at heights (a) 10m, (b) 30m, and (c) 50m, at Ali Al-Gharbi Iraq.

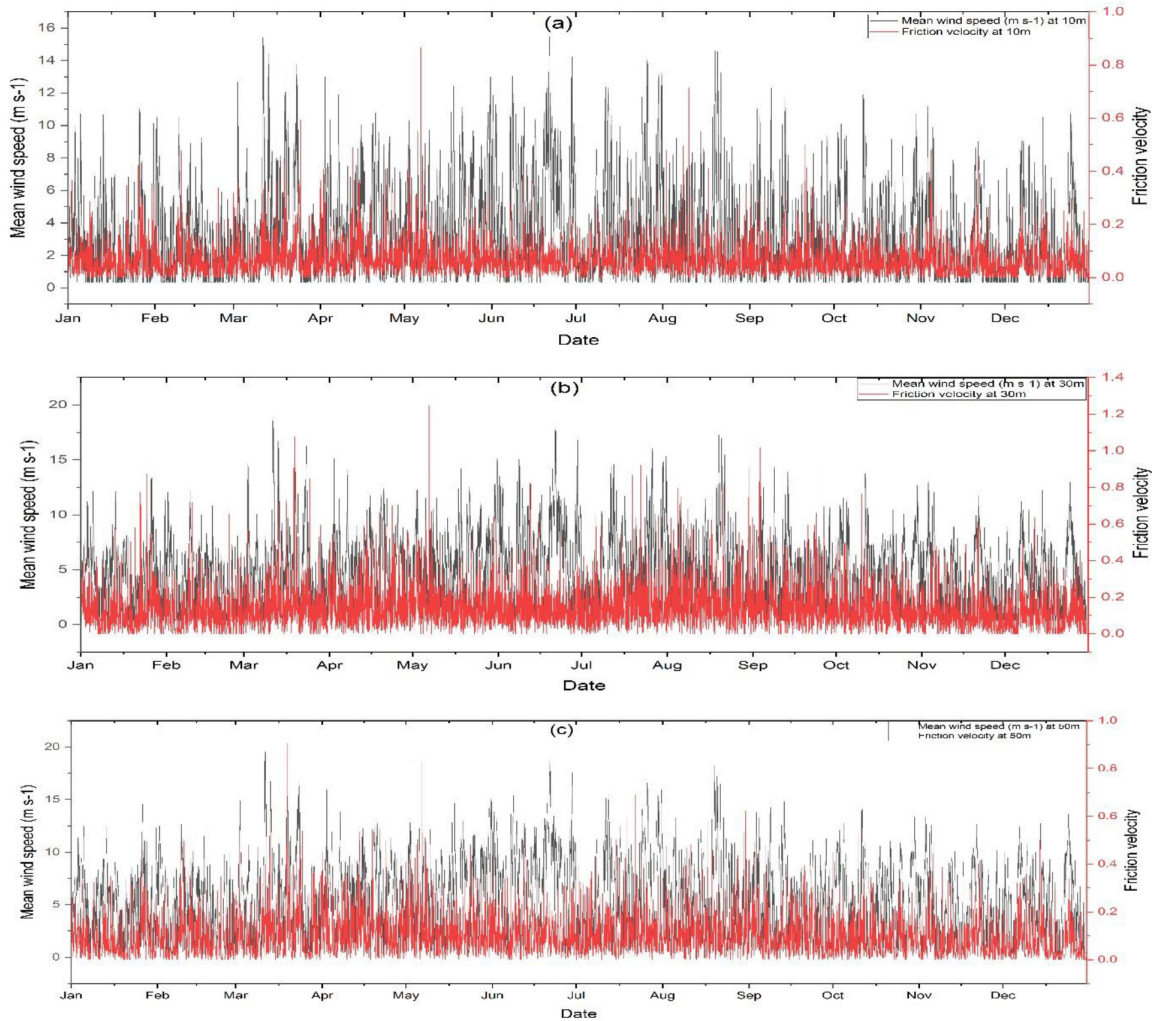


Fig. 4: Time series of horizontal wind speed and friction velocity (eddy wind velocity) at heights (a) 10m, (b) 30m, (c) 50m.

large fluctuation in recorded vertical wind, there are large values of surface heat flux (Fig. 5 a) in April and autumn. On the other hand, also large value of vertical velocity acceleration (w') will have an

especially important maximum record to surface sensible heat flux ($w'T'$) (Fig. 5 b). The effect of the horizontal wind speed value with height can be seen in Fig. 6 (a & b).

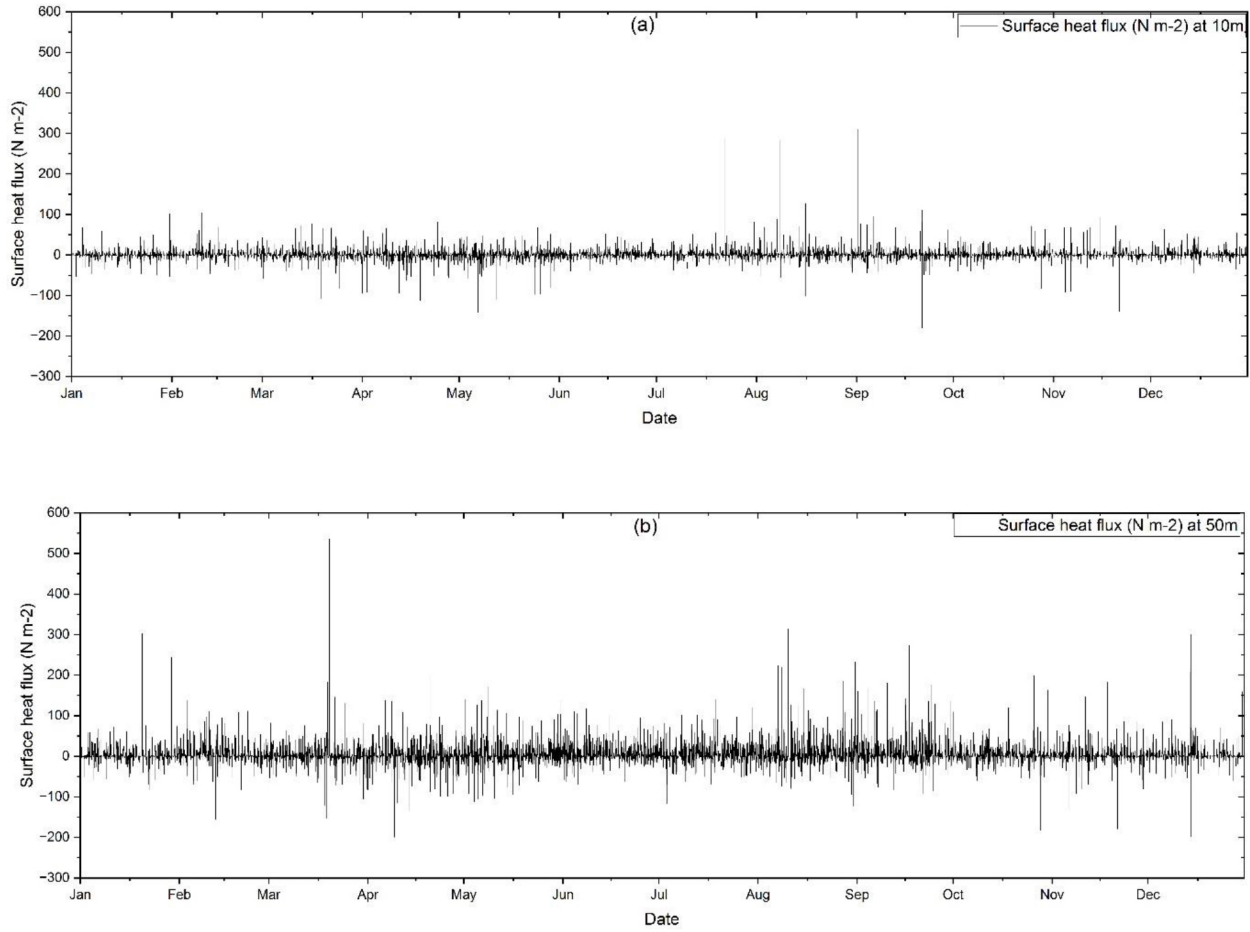


Fig. 5: Surface sensible heat flux at daytime and nighttime at (a) 10m and (b) 50m.

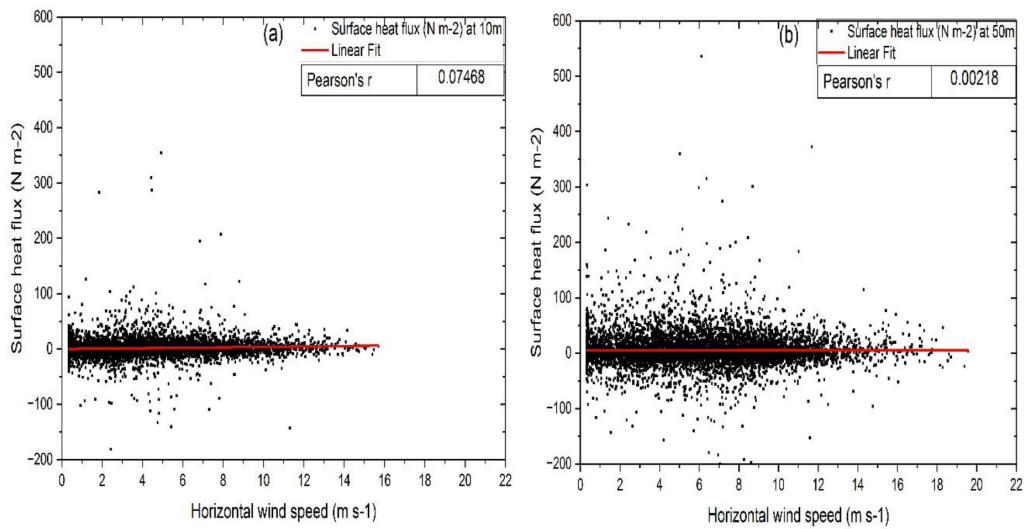


Fig. 6: Relationship between surface sensible heat flux and horizontal wind speed at (a) 10m and (b) 50m.

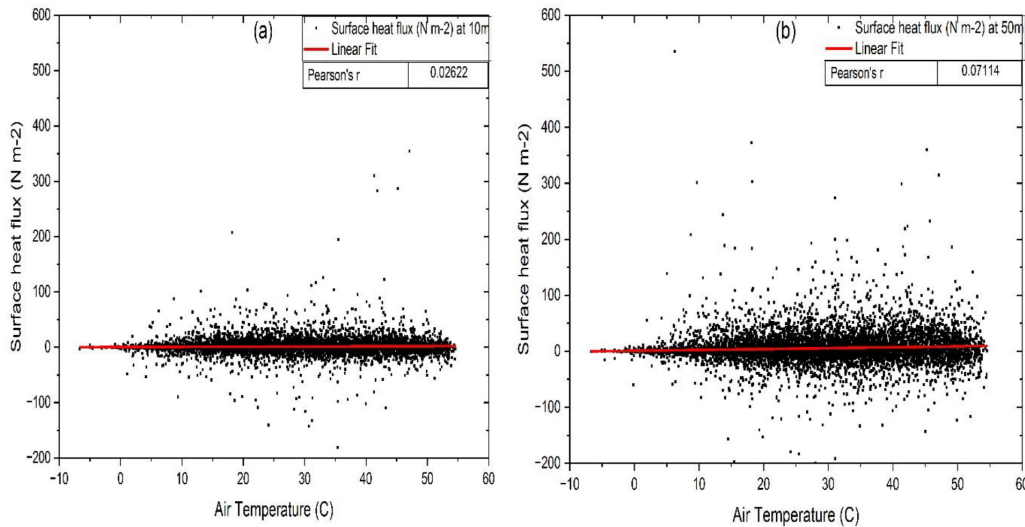


Fig. 7: Relationship between surface sensible heat flux and air temperature recorded at (a) 10m and (b) 50m.

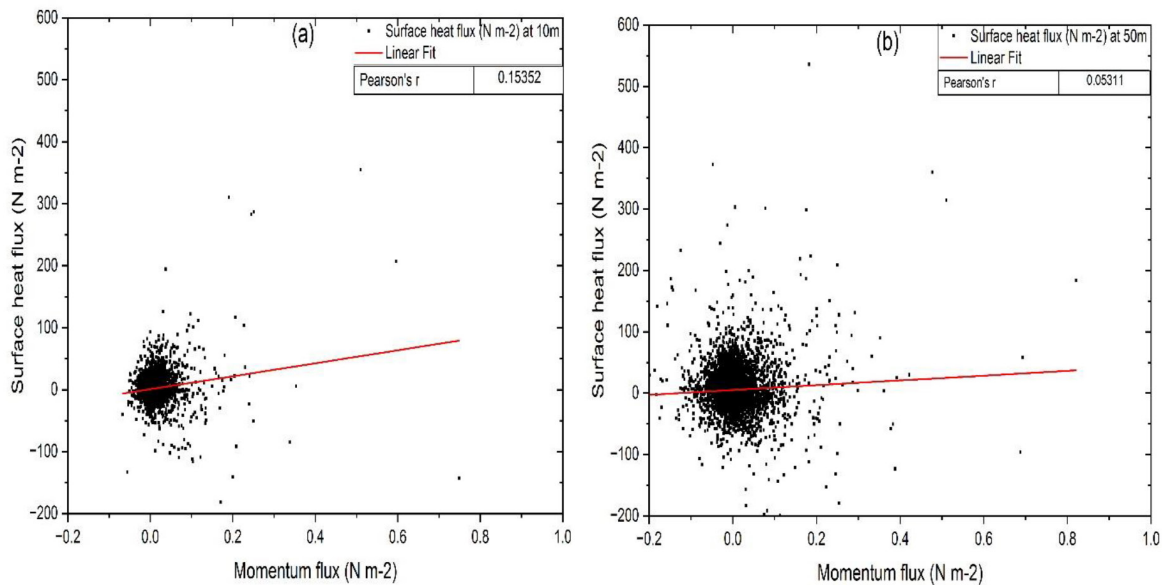


Fig. 8: Relationship between surface sensible heat flux and momentum flux at (a) 10m and (b) 50m.

Fig. 7 shows the effect of air temperature on the surface heat flux. At low temperatures, the surface heat flux values are small and when temperature increases and instability increases, the surface heat flux becomes large. The surface heat flux values were $1.3 \pm 15.1 \text{ N m}^{-2}$ and $53 \pm 28.4 \text{ N m}^{-2}$ at 10m and 50m respectively (Fig. 7 a & b). It's taken high values at a high level relative to a height near to the ground. Air temperature near the ground has a significant effect on activation of air temperature that enlarges with eddy motion.

Relationship between momentum flux and surface heat flux

In the atmospheric boundary layer two forces are important from stability point of view. The first one is the horizontal force or mechanical force that act in the horizontal direction and referred to

as momentum flux ($u'w'$), The second one is the convection force that actions in vertically and represents the most buoyancy force of air mass that moves upward and downward because it is bouncy relative to the environment. In Fig. 8 (a, b) momentum flux ($u'w'$) is plotted in against surface heat flux at height (a) 10m and (b) 50m. At 10m vertical flux force ($w'T'$) is so active relative to horizontal force ($u'w'$), the relation coefficient is 0.2, this refers to the activity of ground heating and buoyancy of air near the ground. Momentum flux at 10m has values ranging from -50 to $+100 \text{ N m}^{-2}$, and most momentum flux in values are within $\pm 0.05 \text{ m}^2 \text{ s}^{-2}$ range at 50m. Thus, most momentum flux be in range from -80 to $+100 \text{ N m}^{-2}$, and momentum flux in range $\pm 0.150 \text{ m}^2 \text{ s}^{-2}$. There is large dispersion in data at 50m more than that at 10m because increase horizontal force and enlarged the eddy motion, far from earth ground, and roughness element.

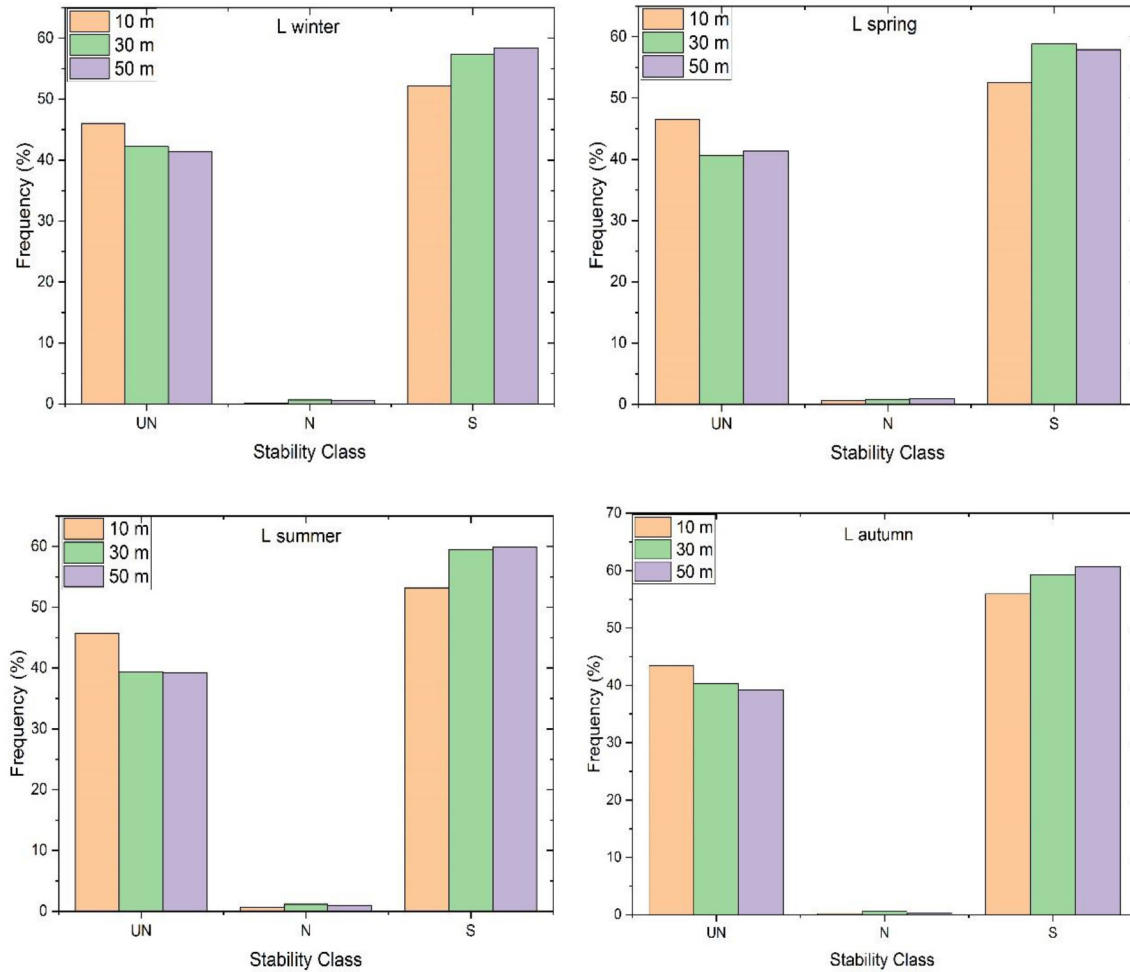


Fig. 9: Monin-Obukhov length frequency values at heights 10m, 30m, and 50m during winter, spring, summer, and autumn seasons

Monin-Obukhov length (L)

The momentum and heat flux deals with the two forces acting in the atmosphere, one action in the horizontal and second vertical direction. The two forces determine atmospheric stability in the atmospheric surface layer. Monin-Obukhov considers very important indices in the surface boundary layer, referring to positive and negative signs values and zero, all these indicate stability, at different heights, where the horizontal and vertical force (momentum and heat flux) change. Fig. 9 (a,b,c,d) shows the behavior of (L) values according to seasons. During the daily cycle, three cases of atmospheric stability appear to us, during daytime hours, weather conditions are often unstable, while during the night hours stable weather conditions dominate, while neutral weather conditions are a transitional state between stable and unstable weather conditions (an hour after sunrise and an hour before sunset). It shows unstable conditions more than in seasons summer and autumn, while neutral conditions decrease to small values at autumn season. The stability index (z/L) is also calculated according to a height of measurement at 10m and 50m. Fig. 10 shows the relationship between stability index (z/L) at heights 10m and 50m and momentum flux (τ), it has large values of momentum flux concentrated in the neutral conditions. While at unstable conditions (negative z/L), and stable

conditions (positive z/L) the momentum flux has a small value. The relationship between heat flux or sensible heat flux with stability index (z/L) are explained in Fig. 11 (a & b). The large values of heat flux are found in neutral conditions but the difference in the heat flux is positive in the stable conditions (+ z/L) and negative in the unstable conditions (- z/L).

Effect of Monin-Obukhov length (L) on wind energy density (E)

Table 2 shows the mean wind speed, wind power density, and wind energy density at two heights (30m and 50m), for different states of atmospheric stability (Stable (S) Unstable (UN), and Neutral (N)). In the Neutral (N) atmospheric conditions, the highest values of mean wind speed and wind power density were (6.2 m s^{-1} - 142.9 W m^{-2}) at a height of (30 m). While at the height of (50 m), the highest values of mean wind speed and wind power density were (7.1 m s^{-1} - 214.7 W m^{-2}), but the lowest seasonal frequencies occurred in the conditions of neutrality for all heights, and the frequency rate was approximately 1%. In the Unstable (UN) atmospheric conditions, the lowest values of mean wind speed and wind power density were (4.4 m s^{-1} - 51.1 W m^{-2}) at a height of (30 m). In height (50 m), the lowest values of mean wind speed and wind power density were (5.1 m s^{-1} - 79.5 W m^{-2}). According to Stable (S)

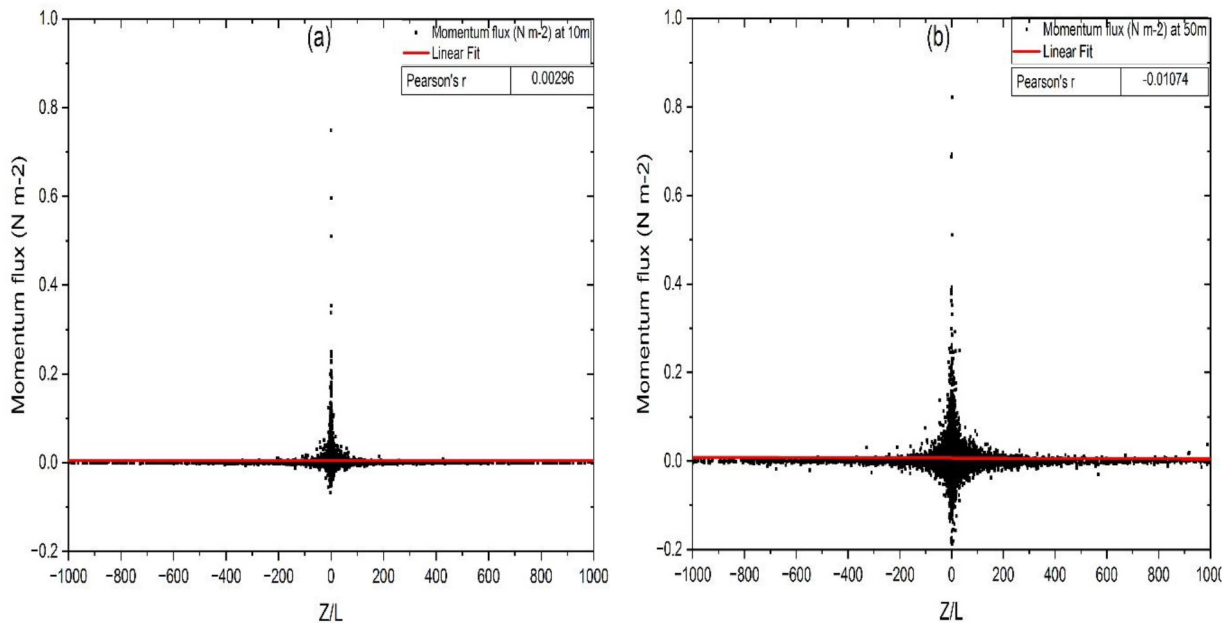


Fig. 10: Relationship between stability index (z/L) and momentum flux at (a) 10m and (b) 50m.

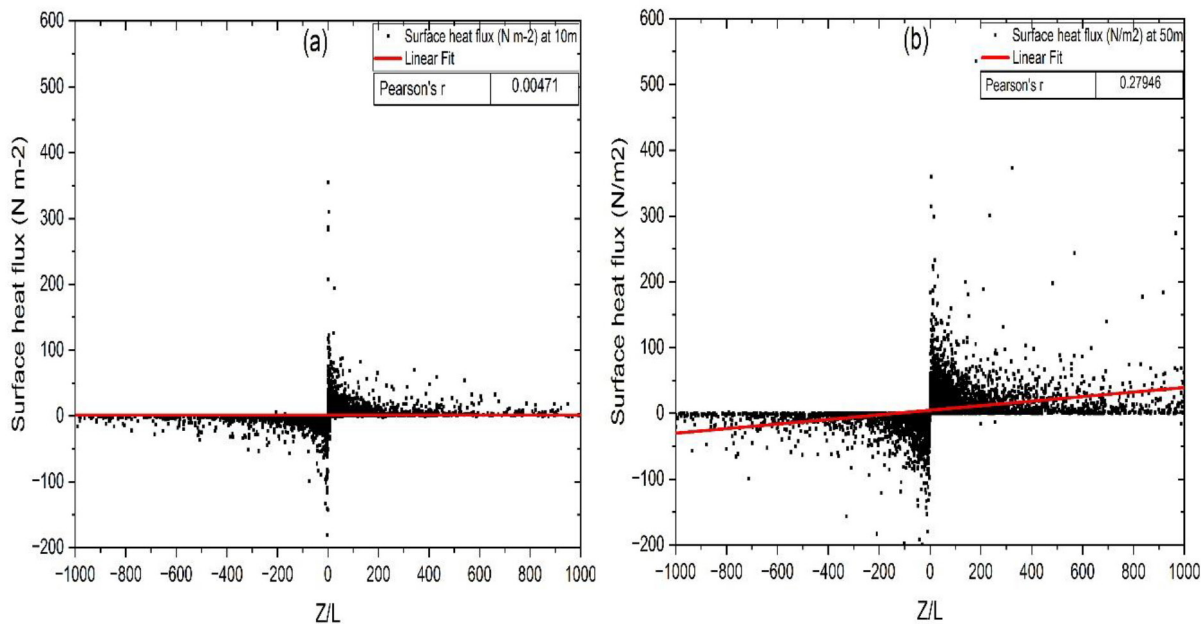


Fig. 11: Relationship between stability index (z/L) and surface heat flux at (a) 10m and (b) 50m.

atmospheric conditions, the lowest values of mean wind speed and wind power density were ($6.1 \text{ m s}^{-2} - 136.1 \text{ W m}^{-2}$) at a height of (30 m). While at the height of (50 m), the lowest values of mean wind speed and wind power density were ($6.8 \text{ m s}^{-2} - 188.6 \text{ W m}^{-2}$). The highest wind energy density in sable atmospheric conditions was ($238079.2 \text{ W m}^{-2} \text{ h}^{-1} - 174778.2 \text{ W m}^{-2} \text{ h}^{-1}$) with percentage (58% - 57%) in the spring season at both heights, respectively, while the lowest wind energy density in neutral atmospheric conditions was ($1421.3 \text{ W m}^{-2} \text{ h}^{-1} - 1502.5 \text{ W m}^{-2} \text{ h}^{-1}$) with percentage (1.3% - 0.8%) in autumn season at both heights, respectively. From the results of the table, it can be concluded that the highest wind energy density

was in stable conditions, followed by unstable conditions. While in neutral conditions, wind energy density was the lowest due to its extremely low frequency in all seasons.

CONCLUSIONS

This study evaluated atmosphere stability using the Monin-Obukhov length method and the analysis revealed that the vertical wind speed exhibits a rise until reaching a height of 30 m, after which it experiences a drop at 50 m. Conversely, the horizontal wind speed shows a positive correlation with increasing height. The values of frictional velocity exhibit significant fluctuations,

Table 2: Seasonal variation of wind speed (m s^{-2}), wind power density (W m^{-2}), and wind energy density ($\text{W m}^{-2} \text{h}^{-1}$) at two heights (30 m - 50 m) under three stability classes

Seasons	Stability class	Height 30m			Height 50m		
		Wind speed (m s^{-2})	Wind power density (W m^{-2})	Wind energy density ($\text{W m}^{-2} \text{h}^{-1}$)	Wind speed (m s^{-2})	Wind power density (W m^{-2})	Wind energy density ($\text{W m}^{-2} \text{h}^{-1}$)
Winter	UN	4.4	51.1	46578.5	5.1	79.5	100112.7
	N	5.9	123.2	1596.6	6.6	172.9	2240.7
	S	4.6	58.4	72280.5	5.2	84.3	75202.3
Spring	UN	6.1	136.1	120679.8	6.8	188.6	170526.4
	N	6.2	142.9	2079.1	6.3	150.1	2949.4
	S	6.1	136.1	174778.2	6.8	188.6	238079.2
Summer	UN	4.9	70.5	61331.4	5.7	111.1	95914.8
	N	5.4	94.4	2292.1	6.1	136.6	2714.2
	S	5.1	79.5	104268.2	5.7	111.1	146694.2
Autumn	UN	4.4	51.1	45469.8	4.8	66.3	88712.1
	N	6.1	136.1	1502.5	7.1	214.7	1421.3
	S	4.4	51.1	66794.3	5.3	89.3	77094.4

Note: UN-Unstable, N- neutral, and S- stable

making their relationship with horizontal wind speed unclear. Elevated magnitudes of vertical and horizontal wind velocities influence the highest magnitudes of surface heat flux. The surface heat flux values are influenced by the air temperature, with higher air temperatures resulting in larger surface heat flux. The surface heat flow gets stronger compared to the momentum flux at a height of 10 m, however, the situation is reversed at a height of 50 m. The occurrence of stable weather conditions is most prevalent across the four seasons, followed by unstable and neutral situations. The highest frequency (59%) occurred in stable atmospheric conditions followed by unstable conditions (40%) at heights of 50m. The lowest frequency (1%) occurred in neutral atmospheric conditions. The highest wind energy density was in stable conditions with a percentage 58% - 57% in the spring season at both heights, respectively, followed by unstable conditions. While the highest wind energy density was in neutral conditions with a percentage (1.3% - 0.8%) in the autumn season at both heights respectively, wind energy density was the lowest due to its exceptionally low frequency in all seasons. The highest monthly values of wind power density and wind energy density can be noticed in June and July, and the lowest values can be observed in January and February. Therefore, the summer has a higher wind power density than other seasons. Thus, it is significant to consider atmospheric stability conditions when estimating wind energy at a site to prevent errors in energy production estimates.

ACKNOWLEDGMENTS

The authors would like to thank and appreciate the Iraqi Ministry of Science and Technology for providing the necessary data for this research.

Conflict of Interests: The authors declare that there is no conflict

of interest related to this article.

Funding: The authors did not receive support from any organization for the submitted work.

Data availability: Wind speed, direction, and temperature data for the year 2017 were obtained from the Iraqi Ministry of Science and Technology, Department of Renewable Energy, through the meteorological tower installed in the study area (Ali al-Gharbi) and stored in their repository.

Author contribution: **J. M. Khadir:** Data checked, processed, analyzed, and presented, Investigation, Writing-original draft; **A. F. Hassoon:** Supervision, writing review, and editing; **B. A. Al-Knani:** Supervision.

Disclaimer: The contents, opinions and views expressed in the research article published in the Journal of Agrometeorology are the views of the authors and do not necessarily reflect the views of the organizations they belong to.

Publisher's Note: The periodical remains neutral with regard to jurisdictional claims in published maps and institutional affiliations

REFERENCES

- Abdalla, A., El-Osta, W., Nassar, Y.F., Husien, W., Dekam, E.I. and Miskeen, G.M. (2023). Estimation of Dynamic Wind Shear Coefficient to Characterize Best Fit of Wind Speed Profiles under Different Conditions of Atmospheric Stability and Terrains for the Assessment of Height-Dependent Wind Energy in Libya. *Appl. Energy*, 59: 343-359. doi.org/10.3103/s0003701x23600212
- Al-Knani B. A. (2015). Turbulence Intensity Calculation of Al-

- Sulaimaniyah Province in Iraq. *Al-Mustansiriyah J. Sci.*, 26 (2): 78-83. <https://www.iasj.net/iasj/article/111601>
- Fiorillo, E., Brilli, L., Carotenuto, F., Cremonini, L., Gioli, B., Giordano, T. and Nardino, M. (2023). Diurnal Outdoor Thermal Comfort Mapping through Envi-Met Simulations, Remotely Sensed and in Situ Measurements. *Atmosphere* 14: 641. doi.org/10.3390/atmos14040641
- Foken T. and Mauder M. (2024) *Micrometeorology*. Springer International Publishing AG, p410. <http://books.google.ie/books>
- Göçmen, T., Laan, P. van der, Réthoré, P.-E., Diaz, A.P., Larsen, G.Ch. and Ott, S. (2016). Wind turbine wake models developed at the technical university of Denmark: A review. *Renew. Sustain. Energy Rev.*, 60:752-769. doi.org/10.1016/j.rser.2016.01.113
- Hadi, F.A., Abdulsada Al-Knani, B. and Abdulwahab, R.A. (2020). An assessment the wind potential energy as a generator of electrical energy in the coastal area of southern Iraq. *Sic. Rev. Eng. Environ. Sic.*, 29: 37-53. doi.org/10.22630/pniks.2020.29.1.4
- Hassan, Q., Viktor, P., J. Al-Musawi, T., Mahmood Ali, B., Algburi, S., Alzoubi, H.M., Khudhair Al-Jiboory, A., Zuhair Sameen, A., Salman, H.M. and Jaszczur, M. (2024). The renewable energy role in the global energy Transformations. *Renew. Energy Focus.* 48:100545. doi.org/10.1016/j.ref.2024.100545
- Hassoon A. F. and Roomi T. O. (2023). Effect of the Convective Boundary Layer on Radiosonde Flight Path Over Baghdad Airport Station (Case Study). *Iraqi J Agric. Sci.*, 54: 1603-1621. doi.org/10.36103/ijas.v54i6.1861
- Hassoon, A. and Al-Dabbagh, S. (2023). Effect Dynamic Stability of Atmospheric Boundary Layer on Plume Downward Flux Emitted from Daura Refinery Stacks. *Iraqi Geology. J.* 56: 161-171. DOI: 10.46717/igj.56.1A.12ms-2023-1-24
- Holtslag, M.C., Bierbooms, W.A.A.M., Bussel, G.J.W. van, (2014). Estimating atmospheric stability from observations and correcting wind shear models accordingly. *J. Phys.*, 555: 012052. doi.org/10.1088/1742-6596/555/1/012052
- Kumar P. (2022). *Mechanics of Materials*. Indian Institute of Technology Kanpur, p544. <http://books.google.ie/books>
- Morrison, T., Calaf, M., Higgins, C.W., Drake, S.A., Perelet, A., Pardyjak, E., (2021). The Impact of Surface Temperature Heterogeneity on Near-Surface Heat Transport. *Bound-Layer Meteor.*, 180: 247-272. doi.org/10.1007/s10546-021-00624-2
- Munjong N. E., (2022). The Transition of Fossil Fuel as A Source of Energy to Renewable Energy. MSC [Thesis]. Finland: Centria University of Applied Sciences. <https://urn.fi/URN:NBN:fi:amk-202203284086>
- Nwaigwe, K.N., (2021). Assessment of wind energy technology adoption, application and utilization: a critical review. *Inter. J. Environ. Sci. Techno.*, 19, pp 4525-4536. doi.org/10.1007/s13762-021-03402-2
- Pérez, C., Rivero, M., Escalante, M., Ramirez, V., Guilbert, D., (2023). Influence of Atmospheric Stability on Wind Turbine Energy Production: A Case Study of the Coastal Region of Yucatan. *Energies* 16: 4134. doi.org/10.3390/en16104134
- Phillips, D.P., Hopkins, F.E., Bell, T.G., Liss, P.S., Nightingale, P.D., Reeves, C.E., Wohl, C. and Yang, M. (2021). Air-sea exchange of acetone, acetaldehyde, DMS and isoprene at a UK coastal site. *Atmos. Chem. Phys.*, 21: 10111-10132. doi.org/10.5194/acp-21-10111-2021
- Radünz, W.C., Sakagami, Y., Haas, R., Petry, A.P., Passos, J.C., Miqueletti, M. and Dias, E. (2020). The variability of wind resources in complex terrain and its relationship with atmospheric stability. *Energy Convers Manag.*, 222: 113249. doi.org/10.1016/j.enconman.2020.113249
- Resen A. K. (2023). Wind Resource Estimation and Mapping at Ali Al-Gharby Site (East-South of Iraq) Using WAsP Model. *Iraqi J. Sci.* 56(2A): 1216-1223. <https://www.ijis.uobaghdad.edu.iq/index.php/eijs/article/view/10272>
- Roomi T. (2000). Estimation of the vertical description of the wind speed and temperature within the lowest hundred meters above Baghdad. MSC [Thesis]. Iraq: Mustansiriyah University. doi:10.13140/RG.2.2.13302.73287
- Singh, P., Singh, S., Kumar, G. and Baweja, P. (2021). *Energy*. John Wiley & Sons. <http://books.google.ie/books>
- Stiperski, I. and Calaf, M. (2023). Generalizing Monin-Obukhov Similarity Theory (1954) for Complex Atmospheric Turbulence. *Phys. Rev Lett.* 130(12): 124-132. doi.org/10.1103/physrevlett.130.124001